Assessing Hyperloop Transport Capacity Under Moving-Block and Virtual Coupling Operations

Borges, Rafael Mendes; Quaglietta, Egidio

DOI
10.1109/TITS.2021.3115700

Publication date
2021

Document Version
Accepted author manuscript

Published in
IEEE Transactions on Intelligent Transportation Systems

Assessing Hyperloop Transport Capacity Under Moving-Block and Virtual Coupling Operations

Rafael Mendes Borges and Egidio Quaglietta

***Abstract*— The Hyperloop is a concept of a ground transportation system consisting of capsules traveling at very high-speeds in near-vacuum tubes. The Hyperloop aims to be a fast, cheap, and sustainable alternative to short-haul flights and high-speed rail. The small pod size requires very high frequencies to respond to future high levels of passenger and cargo demands. Media and representatives of the emerging Hyperloop industry acclaim the Hyperloop as a very capacity effective transport system, however there is no clear scientific evidence proving that. A theoretical investigation is therefore necessary to understand which capacity the Hyperloop could safely provide. This paper provides a comparative analysis of the capacity that the Hyperloop can offer for several operational scenarios and different signalling systems, including Moving-Block and the advanced concept of Virtual Coupling. Results show that Moving-Block could achieve required transport capacity levels only if pods could use high deceleration rates likely to be unsafe and uncomfortable to passengers. Virtual Coupling is instead observed to be a more satisfactory operational concept that could provide a higher transport capacity while respecting safety and comfort standards if reliable pod platooning technologies are available.**

***Index Terms*— High-speed transport, Hyperloop capacity, moving-block, virtual coupling.**

I. Introduction

THE Hyperloop is a conceptual mode of transport in which pods travel at very high-speeds in a reduced pressure tube. The proposed concept is claimed to achieve better performances in terms of travel time, costs, energy consumption and safety when compared to short-haul flights and high-speed rail [1]. The development of the Hyperloop concept is still at an early stage. It is still unknown when the concept will become a reality or even when a full-scale test will take place. One of the most relevant experiences so far was conducted by Virgin Hyperloop in November 2020. This was the first time a test involved passengers (only four people travelled inside the pod), in a short trip where the speed of the experimental pod did not exceed 48 m/s [2].

The Hyperloop has been reported [1] as a very capacity-effective system, despite there is no scientific evidence for that statement. Vehicles to be used in the Hyperloop will have a limited size to fit the tube meaning a reduced vehicle capacity to accommodate passengers and/or cargo. Because of the restricted vehicle capacity, the Hyperloop shall rely on high frequencies to respond to the expected travel demand growth of passengers and freight. Different values for the probable future transport demand of the Hyperloop are referred in the literature. Musk [1] forecasts a demand of 6 million pax/year for the link between Los Angeles and San Francisco/San Jose. This volume corresponds to a maximum of approximately 15,000 pax/day and direction [3]. Another example is given by Hansen [3], that estimates a demand of 10,000 pax/day and direction based on air transport between major German and European airports. A deeper theoretical capacity investigation is hence needed to understand the actual transport capacity of the Hyperloop when realistic operational scenarios and safety constraints of the signalling system are considered.

Few studies exist about Hyperloop capacity analysis. Musk in the Hyperloop Alpha paper [1] reports that pods would depart regularly every two minutes, and the inter-departure time can be decreased to 30 s during peak hours. Decker *et al.* [4] compute the maximum safe pod frequency based on an absolute braking distance separation and assuming a deceleration rate of 1g, which leads to a minimum inter-departure time of 30 s. Another interesting work was made by van Goeverden *et al.* [5] who perform a multi-criteria analysis indicating the Hyperloop as a premium transport mode given that the limited capacity would make ticket prices only affordable by exclusive passenger categories. Their conclusion however relied on a macroscopic capacity model that disregarded possible pod manoeuvres at junctions and detailed safety constraints due to the signalling system. They report an interval between departures of five minutes, based on a deceleration rate of $\sim$0.15g.

Some of the pod frequencies found in the literature report promising values. However, the high deceleration rates considered are likely to be unsafe and uncomfortable for the passengers. Powell and Palacín [6] refer to the importance of the acceleration and jerk rates for passenger safety and comfort. Results from the study show that from longitudinal accelerations of 1.5m/s^2 there is a steep increase of passenger discomfort even if jerk rates are minimal. Moreover, there is no clear evidence if there will be advances in technology to safely achieve those reported deceleration rates. Furthermore, the existing literature on transport capacity of the Hyperloop system has been focused only on the simple case of plain lines

Manuscript received September 11, 2020; revised March 21, 2021 and August 1, 2021; accepted August 27, 2021. The Associate Editor for this article was M. Zhou. *(Corresponding author: Rafael Mendes Borges.)*

Rafael Mendes Borges was with the Department of Transport and Planning, Delft University of Technology, 2628 CN Delft, The Netherlands (e-mail: rf.brgs@gmail.com).

Egidio Quaglietta is with the Department of Transport and Planning, Delft University of Technology, 2628 CN Delft, The Netherlands (e-mail: e.quaglietta@tudelft.nl).

Digital Object Identifier 10.1109/TITS.2021.3115700

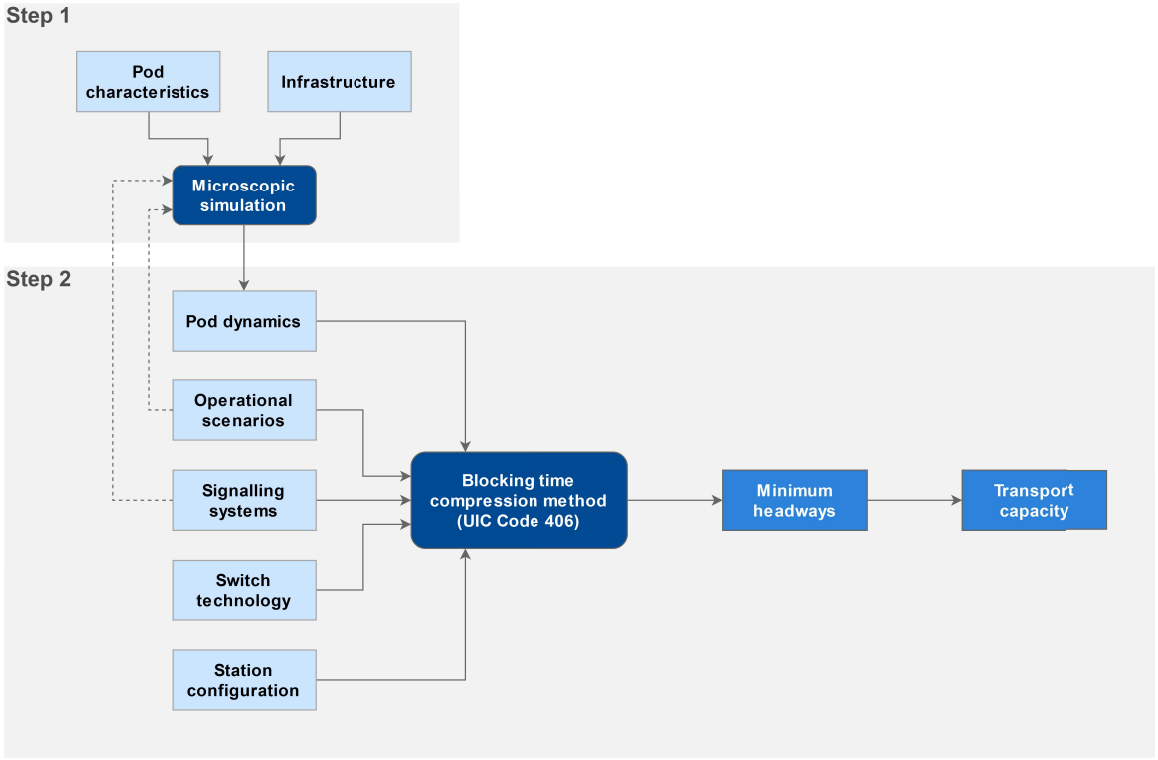

Fig. 1. Overview of the methodology used to assess the Hyperloop transport capacity.

excluding intermediate stops or junctions where multiple pods could merge/diverge. The actual Hyperloop transport capacity might hence be much lower than what has been so far reported if realistic pod manoeuvres at junctions/stations as well as safe signalling constraints are taken into account.

Existing literature has mostly assumed a separation between consecutive pods to be at least the absolute braking distance, i.e. the distance required for a capsule to brake from its current speed to standstill, although without specifying the type of signalling technology to achieve that separation. Even so, such a concept resembles Moving-Block (MB) operations already used in metro lines by means of the Communication Based Train Control (CBTC) [7] and specified for conventional railways by the ETCS Level 3 standard (not yet been implemented) [8]. The reported high pod frequencies rely on high deceleration rates to brake in case the pod ahead suddenly stops. However, an advanced signalling concept known as Virtual Coupling (VC) has been proposed in the railway field in which vehicles could follow each other at distances shorter than the absolute braking distance to eventually move synchronously in radio-linked platoons which could be treated as a single vehicle [9]. Under VC pods could hence couple/decouple on-the-run by first following each other at a relative braking distance (i.e. the distance to brake from current speed to the speed of the pod ahead) until they synchronize their speed with the pod ahead to form a platoon. Pods moving in a platoon are separated only by a safety margin which depends on the running speed and the difference in braking rates of the pods. Such a concept might represent an attractive alternative to achieve satisfactory pod frequencies while keeping deceleration rates at levels that are safe and respect passenger comfort.

In this work, our approach is based on the most advanced concepts from the railway industry, such as MB and VC. However, other studies present alternative solutions that can be used for parts of the same problem. For example, Gao *et al.* [10] proposes a strategy for automatic train operation of high-speed trains based on control theory. Chen *et al.* [11], in turn, presents a strategy to optimize the capacity of high-speed railway networks by geographically rebalancing the capacity utilization of the network.

This paper aims to cover the existing gap in the literature by assessing the transport capacity which the Hyperloop can safely provide for all possible operational scenarios under both MB and VC signalling concepts.

II. Hyperloop Capacity Assessment Methodology

A two-step methodological framework has been set up (Fig. 1) to assess the Hyperloop transport capacity for several pod manoeuvres on different infrastructure layouts, signalling and switching technologies as well as station configurations.

In the first step, a detailed analysis of pod dynamics is performed. In particular, the microscopic railway traffic simulation tool EGTRAIN [12] has been extended to model Hyperloop pod dynamics and accurately describe pod braking curves. The adaptation of EGTRAIN has been possible due to its flexibility in simulating rail-bound transport systems in general. We modified some of the motion equations originally included in EGTRAIN. Specifically, we have used

pod-specific resistance parameters, increased the maximum achievable speeds, and added an extra equation to take into account the reduced air drag of the pod within a vacuumed tube. The traditional rolling resistance due to train wheels rolling on the rail track has been instead substituted with equations considering the magnetic drag as those adopted for maglev [13]. The tractive effort-speed curve of a standard train has been modified by using specific linear motor propulsion thrust for the pod [13]. In addition, we have modified the constant braking rate originally used for trains in EGTRAIN with a reversed-thrust braking effort for the pod. With the modifications described above, the EGTRAIN simulation model was able to provide more accurate pod dynamics than a simple trapezoidal speed-time profile, resulting therefore in more accurate capacity figures. The inputs to the microscopic model include characteristics of the capsule (e.g. length, mass, tractive effort speed curve) as well as the infrastructure (e.g. track length, gradient, curvature radii).

The second step draws on detailed pod dynamics computed in Step 1 to implement an analytical capacity assessment method to assess Hyperloop capacity for different configurations of the system. Specifically, the analytical assessment builds on the UIC Code 406 blocking time compression [14] which is a consolidated method in the railway field for the evaluation of infrastructure occupation. Capacity is here assessed in terms of the minimum time headway that can be safely allowed between two consecutive pods for each of the following system configurations which constitute an input to the model:

- Operational scenarios: which define a set of possible pod manoeuvres on relevant network locations such as plain Hyperloop tracks, merging and diverging junctions. Operational scenarios also include two different service patterns of i) pods having intermediate stops along the track as well as ii) non-stopping pods only delivering a direct end-to-end connection between the terminal stations of the Hyperloop corridor.
- Signalling systems: where both MB and the advanced signalling concept of VC are considered.
- Direction switching technologies: including two different systems allowing a direction change at merging/diverging junctions. Specifically, the considered systems are a traditional mechanical moving switch and an innovative fixed magnetic switch concept [15].
- Station layout: for the operational scenarios with stops, the capacity is assessed for the case where intermediate stations have one single airlock but also when an airlock for each pod is available, in which case pods can load/unload customers at the same time.

The developed analytical model provides as output the minimum time headway between two consecutive pods for each configuration of the system, i.e. a given combination of operational scenario, signalling system, switching technology and station layout. Obtained minimum headways are then translated in terms of transport capacity and provided as both maximum hourly number of pods and passengers that could be transported. Transport capacity results produced by our framework are then compared with alternative modes of transport, namely high-speed railways and air passenger transport.

A detailed description of inputs/outputs and methods employed is provided in the following subsections.

A. Capsule Dynamics

The simplest approaches to model the capsule dynamics assume constant acceleration and deceleration rates. To obtain more realistic results, this work considers a detailed description of the propulsion system and motion resistances of the pods. The fact the Hyperloop is still a concept has led to many different concepts for its various components. The propulsion system is not an exception and various possible configurations can be found in the literature [13], [16]. This work is based on a single configuration which is a magnetically levitated capsule propelled by a linear synchronous motor as proposed by Choi *et al.* [13].

1) Braking Curve: The braking curve of the pod was simulated by extending the EGTRAIN microscopic railway traffic simulation model [12], which is based on a discrete-time solution of Newton's motion differential equations. The speed v and position s of the pod depend on the tractive effort T, motion resistance R, the rotating mass factor ρ and mass of the pod M. The simulation implements a finite-difference integration of Newton's motion formula with time step $t = t_k - t_{k-1}$, where t_k corresponds to the current time. The speed v_k and position s_k are obtained from the following equations [17]:

$$\begin{cases} v_k = v_{k-1} + \dfrac{T\,(k-1) - R\,(k-1)}{\rho M} \cdot t \\ s_k = s_{k-1} + \dfrac{\rho M}{T\,(k-1) - R\,(k-1)} \cdot v_{k-1} \cdot (v_k - v_{k-1})\,. \end{cases} \tag{1}$$

The set of mathematical expressions capturing the train dynamics were adjusted to include the behaviour of the capsule. The model considers the main characteristics of the pod based on the design proposed in [13], namely mass, length, maximum speed, tractive effort speed curve and motion resistances. The motion resistances that depend on speed include aerodynamic drag (tube pressure of 0.001 atm) and magnetic resistance [13]. Two different types of braking are studied: the application of reverse thrust produced by reversing the motor, and the use of a constant braking rate. It is assumed the motor can produce the same thrust in both directions. The reference value used for the case with a constant braking rate is ∼0.25g. Also, an analysis has been performed to identify impacts on the pod's braking curve of different tube gradients considering a slope of $-3‰$, $+3‰$ as well as a flat track (Fig. 2).

2) Simulated Run: In addition to obtaining the braking curve to be used when assessing the transport capacity, the microscopic simulation was utilized to simulate a run of two pods in a representative Hyperloop corridor having a total length of 600 km between two termini stations. The second pod departs 360 s later, which is enough to let the second capsule running without being constrained by the pod ahead.

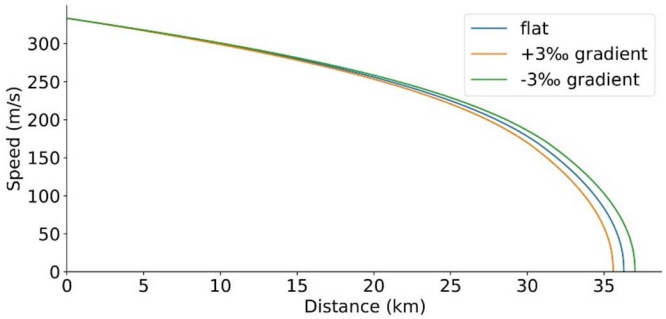

Fig. 2. Pod braking curves for various track gradients, using reverse thrust for braking (reverse thrust at 100%).

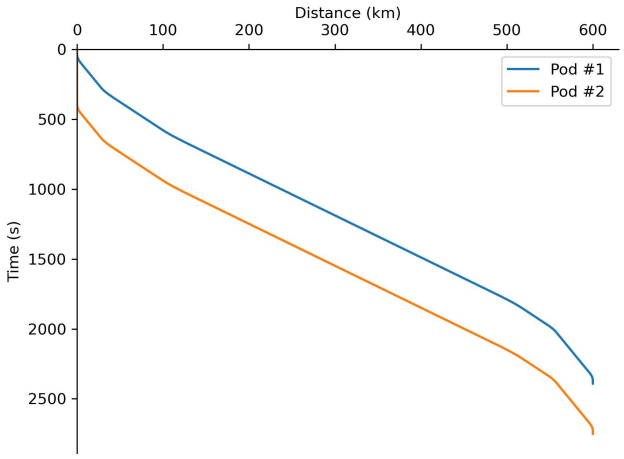

Fig. 3. Time-distance diagram of two pods running in the same tube.

Fig. 3 shows the simulated time-distance diagram of both capsules. The slope of the curves varies along the tube as the maximum speed changes stepwise (480, 890 and 1200 km/h) both at the beginning and the end of the tube.

B. Operational Scenarios

Hyperloop networks will likely consist of links between main cities possibly with intermediate stops and connections to other lines and branches. Junctions allowing pods to merge/diverge from/to different destinations as well as intermediate stations will likely be potential bottlenecks constraining the maximum transport capacity of the Hyperloop. Our study hence analyses different possible types of infrastructure layouts and the corresponding type of vehicle manoeuvres which could be found on a Hyperloop corridor. A combination of infrastructure layout and a manoeuvre is here defined as an operational scenario. A total of six operational scenarios have been defined considering non-stopping and stopping Hyperloop services on a plain line, a merging and a diverging junction (Fig. 4). A similar set of scenarios have been firstly defined by Aoun *et al.* [18] to perform a comprehensive multi-criteria assessment of next-generation train-centric railway signalling systems for different rail market segments. The plain line consists of two consecutive pods traveling in the same direction and the same tube. The second manoeuvre is a merging junction where one of the capsules enters the main tube from a branch. It is assumed the pod coming from the branch crosses the merging junction as first. For the stopping service, both pods stop at the platform located 3 km ahead of the junction. Finally, the diverging junction is a link from the main tube to a branch. For the non-stopping service, the first pod diverges to the branch while the capsule behind continues on the main tube. In the diverging junction with stop, the capsule ahead continues on the main tube and stops at the platform while the pod behind diverges to the branch without stopping. The platform is located 3 km after the junction, in the main tube.

For the merging/diverging junctions, the headways are calculated at the junction. It is assumed a speed limit of 1200 km/h on the main tube, while the speed of the capsule taking the switch depends on the specific switch technology considered. For the plain line without stop, the headway is computed in a section where the speed limit is 1200 km/h. For the plain line with stop, the arrival headway is considered.

In the railways, capacity bottlenecks are commonly due to junctions, as switches are safety critical elements which generally require trains to slow down to avoid derailments. In the case of the Hyperloop, it is not clear which technology will be adopted to let pods switch over merging and diverging tracks. Hardt Hyperloop [15] has introduced the concept of an innovative magnetic switching technology having no moving infrastructure elements, claimed to allow pods changing direction without speed reductions. However, such a technology has not yet been proved on a full-scale test track. Given the nonexistence of a consolidated and proved Hyperloop switching technology, this study will investigate the capacity for both the case of classical mechanical switches with moving beams (as adopted in railways) as well as innovative high-speed fixed magnetic switches. Therefore, pod manoeuvres over diverging and merging junctions consider the existence of two different types of direction switching technologies: i) a Fixed Magnetic Switching technology (FMS) like the one proposed by Hardt [15] which does not require speed reductions and setup times to move and lock the switch, ii) a Moving Mechanical Switch (MMS) like those traditionally used in the railways which requires a given setup time (assumed here to be 4 s) to move, set and lock the switch in the correct direction for the pod. Given that an MMS could fail to move in time and/or in a safe direction between two consecutive pods, an absolute braking distance separation will need to be imposed before this type of switches either under MB or VC at junctions. Taking into account the FMS technology is still in development, this study considers a case without speed reduction but also speed restrictions of 750 km/h and 100 km/h. Regarding the MMS, a single case is studied, where a speed restriction of 100 km/h is imposed as this is the maximum speed currently allowed on traditional mechanical railway switches.

Also, stations are a relevant location when studying capacity. As it happens with switches, the operational conditions at stations are still not clear. Differently from the railways, the Hyperloop will operate in a quasi-vacuumed environment, hence airlocks are needed at stations to let passengers

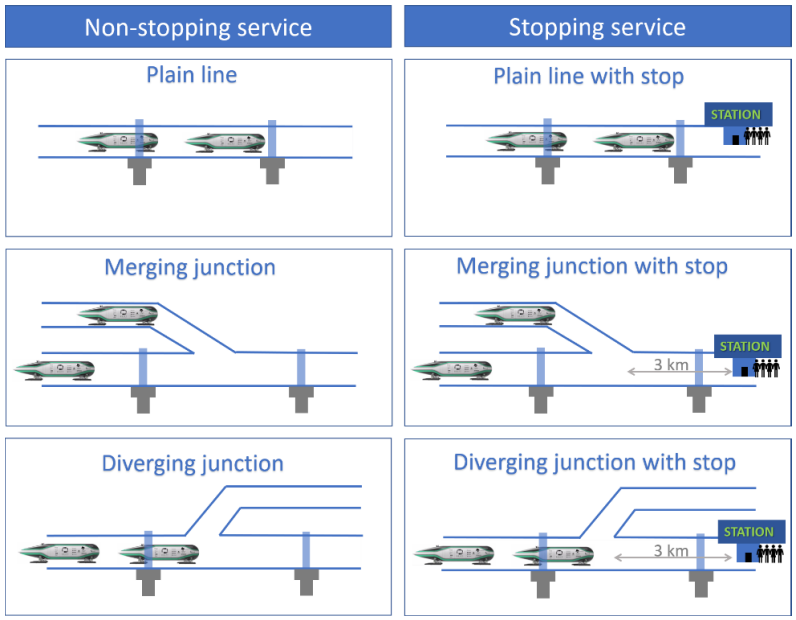

Fig. 4. Schematic operational scenarios to be evaluated.

alight/board the pod while keeping the reduced pressure within the tube [1]. The capacity at stations will be undoubtedly influenced by the number of pods that can embark/disembark passengers and/or cargo at the same time. If no more than one pod is allowed at the same time, the station capacity will be strongly affected. This is very important for the signalling systems considered. For both MB and VC, our capacity investigation assumes two possible cases. For the first case, there is only one chamber so that a platform can be occupied by one single pod, so that if it is occupied, the next pod must wait until the capsule ahead leaves the platform. For the alternative case with two chambers, two pods can stop one behind each other at the same platform to embark/disembark passengers and/or freight while keeping a safe separation of 50 m in between.

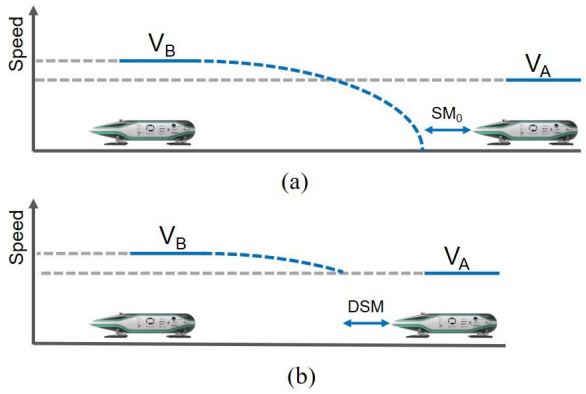

Fig. 5. Pod separation for (a) MB by an absolute braking distance and a fixed safety margin, and (b) VC by a relative braking distance and a dynamic safety margin.

C. Signalling Systems

The Hyperloop will likely build on signalling concepts not far from those currently under investigation in the railway industry given that both are a guideway transport mode. The concept of MB signalling allows consecutive vehicles to be separated by an absolute braking distance (Fig. 5). This way, a vehicle has always enough space ahead to safely stop even if the vehicle ahead suddenly stops. This concept aims at preventing collisions. Additionally, we consider that, under MB, pods keep a fixed safety margin SM_0 that guarantees a minimum separation at standstill.

The proposed concept of VC introduces a Vehicle-to-Vehicle (V2V) communication layer allowing the exchange of speed and acceleration information so that a pod can approach one ahead at a relative braking distance to eventually move synchronously by forming a radio-linked platoon. When traveling in a platoon, pods would keep a safety margin function of the running speed and the difference between braking rates of consecutive pods (Fig. 5). The dynamic safety margin (DSM) applied when pods move under VC is given by:

$$DSM = SM_0 + \max\left(0, \frac{v_l^2}{2b_{f,max}} - \frac{v_l^2}{2b_{l,emerg}}\right) \quad (2)$$

where SM_0 represents the minimum separation at standstill and the second term represents the dependency on the speeds and braking rates of both pods. v_l is the speed of the leading pod, $b_{f,max}$ is the maximum service braking rate of the follower and $b_{l,emerg}$ the emergency braking rate of the leading pod. It is assumed that the emergency braking rate corresponds to 150% of the maximum service braking rate. This additional safety distance guarantees that the follower pod is sufficiently outdistanced from the leading pod in case the latter applies an emergency braking.

Two modes will be evaluated to assess the capacity impacts of VC, namely the Coupling/Decoupling mode ($VC_{C/D}$) and the Platooning mode (VC_P). By default, it is assumed a

capsule is running independently under MB. From there, the transition to the coupling mode happens when a capsule is approaching the pod ahead and the next stretch of their routes is the same. During the coupling mode (VC_C), the capsule behind will try to reach the speed of the pod ahead, always respecting a dynamic safety margin between vehicles. If the pod behind is able to attain the speed of the leading pod, the pods couple and enter the platooning mode (VC_P). This coupled running will last as long as the follower pod is able to follow the leader and while the next stretches of their routes are shared. Whenever the capsules cannot hold these conditions, two possible transitions can happen: unintentional or intentional decoupling. The first happens when the pod behind cannot hold the same speed of the capsule ahead, because of power limitations and/or higher motion resistances, thence the unintentional decoupling mode. After this transition, the follower pod will try to catch up again with the leading pod. If the conditions for platooning are met again, they return to the platooning mode. Thus, it is possible to have multiple transitions between these two modes. The other possible transition from the platooning mode is an intentional decoupling (VC_D). This happens when coupled vehicles approach a diverging junction where the leading pod takes a different route, therefore they cannot run as a platoon anymore. For that reason, the follower capsule intentionally decouples by slowing down until it outdistances by an absolute braking distance from the leader. After an intentional decoupling, the follower pod starts running under MB supervision. If the pod approaches another pod running ahead, then the pod could couple to it and follow the same sequence of state transitions. A complete description of VC operational states and transitions is provided by Quaglietta *et al.* [17].

Given that the pods will reach very high-speeds, they will be driven by an Automatic Train Operation (ATO), regardless of the signalling system used. ATO is even more necessary for operating pods moving in platoons under VC.

D. Blocking Time Compression Method for Capacity Assessment

As already mentioned, the calculation of minimum headways for each system configuration is performed based on an adaptation of the blocking time compression method of the UIC Code 406 [14] which is a consolidated approach in the railway literature. The blocking time theory builds on the concept that a given section of track can be occupied by one and only one vehicle per time. The total time a track section is occupied (and hence blocked) by a pod is the sum of the following terms (Fig. 6):

- Setup time (t_{setup}): the time to set the route. In the case of the Hyperloop, this term will only be included when considering merging/diverging junctions equipped with traditional moving switches where the setup time is the time to move, set and lock a switch in the correct direction for a pod.
- Driving reaction time ($t_{reaction}$): usually the time for the driver to see and react to a signal aspect. Since the Hyperloop is an autonomous system, this term is the ATO reaction time.

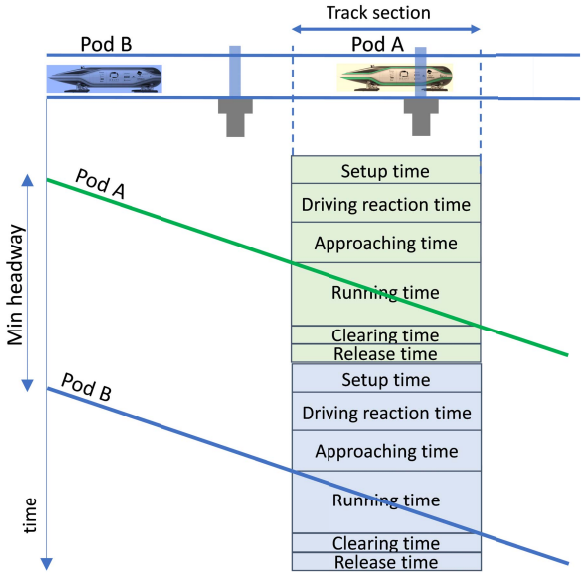

Fig. 6. Method to calculate the time a track section is occupied by a pod.

- Approaching time ($t_{approach}$): the time needed by a pod to approach a given track section ahead. For the Hyperloop, it is the time to cross the safety margin and the absolute or relative braking distance for MB or $VC_{C/D}$, respectively, or the safety margin only for VC_P.
- Running time ($t_{running}$): the time to cross a track section of a given length (called block section in railway literature) which the signalling system supervises so that only one vehicle at a time can occupy it. In the concept of MB operations, the length of a block section becomes infinitesimal since the track section supervised by the signalling system moves along with the vehicle. Such an assumption however does not apply to movable parts of the track such as switches which shall still be considered as fixed block sections. A merging or a diverging pod cannot indeed occupy a switch unless the previous pod has fully cleared it and the switch has been moved, set and locked in the correct position. For this reason, in our model the running time term is only considered over switches but it is assumed to be zero instead on normal tracks.
- Clearing time ($t_{clearing}$): the time needed to clear a block section with the length of the pod.
- Release time ($t_{release}$): the time to release a block section that is considered to be the communication delay to transmit safety-critical information (such as movement authority and/or speed/acceleration of pods) between consecutive pods and/or the ground traffic control centre.

The total time a track section is occupied by a pod, $t_{occupied}$, can be written as:

$$t_{occupied} = t_{setup} + t_{reaction} + t_{approach} + t_{running} + t_{clearing} + t_{release}. \quad (3)$$

As illustrated in Fig. 6, the minimum time headway is therefore identified as the minimum time distance that can be

allowed between two consecutive pods so that their blocking times are not overlapping. Therefore, the minimum time headway between two consecutive pods is:

$$t_{HW} = t^A_{running} + t^A_{clearing} + t^A_{release} + t^B_{setup} + t^B_{driving} + t^B_{approach}, \quad (4)$$

where the superscript represents the first (A) and second (B) pods.

The values used for the setup times depend on the specific type of direction switching technology considered. In particular, the setup time has been assumed to be 4 s if a traditional MMS switching technology is used and 0 if an FMS is instead adopted. This means that in our model a mechanical switch will need 4 s to be moved, set and locked in the right direction for a crossing pod.

The release time is assumed to account for the communication delay to transmit safety critical information. In railway literature [8] about MB, $t_{release} = 2$s is an average time interval between two consecutive updates of the Movement Authority (i.e. the maximum distance a vehicle can safely cross) from a track-side radio control centre to a rail vehicle by using a GSM radio connection. In the case of VC_P instead $t_{release} = 0.02$s can be seen as an optimistic value observed in automotive literature [19] for cooperative vehicles communicating to each other. For VC_C, $t_{release} = 2$s is a reference value since the communication delay accounts for the time needed to receive the Movement Authority from the track-side control centre, operation that occurs in parallel with the V2V communication delay. For this mode, the pod behind needs to exchange kinematics information with the pod ahead. If VC_D then $t_{release} = 2$s is a reference value since the pod behind just needs to receive the Movement Authority from the track-side control centre indicating the location of the diverging switch.

The reference value for the reaction time is assumed to be a constant value $t_{reaction} = 0.5$s in any system configuration. The ATO reaction time is considered independent from a particular system combination of signalling and switching technologies.

The ability to control vehicles at very high-speeds raises concerns about the delay of actuators when implementing control actions resulting from the ATO. Also, studies have shown that the V2V communication between cooperative vehicles has still limitations. The implications of such problems have been investigated, namely on automotive platoons, usually referred to as "string instability" [20], [21]. For that reason, instead of assuming the reference values above, we study a large range of values for both ATO reaction time and communication delay, ranging from the reference values to 8 s.

The values of the approaching and release times depend on the type of signalling and communication system adopted. Specifically, the approaching time is:

$$t_{approach} = \begin{cases} t_{SM_0} + t_{ABD}, & if\ MB \\ t_{DSM} + t_{RBD}, & if\ VC_{C/D} \\ t_{DSM}, & if\ VC_P \end{cases} \quad (5)$$

where t_{ABD} and t_{RBD} are the time to cover the absolute and relative braking distance, respectively, t_{SM_0} the time to cross the fixed safety margin, and t_{DSM} the time to cross the dynamic safety margin. These times are calculated based on the pod dynamics obtained from the microscopic simulations. Whenever possible, pods travel at the maximum allowed speed. The exception is for VC_C, where it is assumed that the leading pod travel with a speed of at most 750 km/h, in order to allow the pod behind to approach the leader.

As mentioned before, in a MB setup, block sections will have an infinitesimal length on the plain track while instead some kind of segregation is still needed at junctions, especially if they are equipped with MMS. In advantage of safety, we also consider that such a segregation at junctions is applied in the case of a FMS, although we assume a null switching time, given that no moving infrastructure elements exist. For this reason, the running time on sections on the plain track will be considered $t_{running} = 0$ (given the infinitesimal length of the section) while it will account for the time to cross the entire length of the switch (assumed to be 100 m for both merging and diverging junctions) at the speed simulated for the pods at the junction.

The clearing time $t_{clearing}$ is instead computed as the time a pod takes to release a section of the track with its entire length (35 m) at the speed simulated for the pods at a given location.

E. Sensitivity Analysis

There is a high level of uncertainty about the possibilities for different technologies to be used by the Hyperloop system. The communication system is one of the various examples, where there is a need to address various challenges [22]. For that reason, it is important to study how changes in the input parameters of our model affect the outcome of our analysis. This justifies the importance of a sensitivity analysis to avoid making hard assumptions in the input parameters.

Our sensitivity analysis uses the One-at-Time (OAT) technique, which is a consolidated method and one of the most common for this type of analysis. Various examples of similar applications of this method can be found in the literature [23], [24]. In the OAT sensitivity analysis, the input parameters are modified one at a time while all other input parameters remain fixed. This way, we study how the output is affected by each change of a given input parameter. For every modification, the relative change from the reference output is given by the partial derivative

$$d_i(X) = \frac{\partial Y}{\partial X_i}, \quad (6)$$

where Y is the output and X_i the input parameter. After testing all the values for a single input parameter, we compute the average of the absolute partial derivatives μ_i,

$$\mu_i = \frac{1}{n}\sum\nolimits_{j=1}^{n} \left| d_i(X^{(j)}) \right|, \quad (7)$$

where n is the sampling space of the input parameters. Finally, we compute the standard deviation for each parameter σ_i,

$$\sigma_i = \sqrt{\frac{1}{n-1}\sum_{j=1}^{n} \left(d_i(X^{(j)}) - \mu_i\right)^2}. \quad (8)$$

TABLE I
MINIMUM TIME HEADWAYS [S] FOR ALL THE COMBINATIONS STUDIED WHEN USING REVERSE THRUST FOR BRAKING

		MB			$VC_{C/D}$			VC_P		
Input Parameter	X_i	Y_i	μ_i	σ_i	Y_i	μ_i	σ_i	Y_i	μ_i	σ_i
Communication delay [s]	**0.02**							179.99	1	0
	0.1							180.07		
	0.5							180.47		
	1							180.97		
	2	227.60	1	0	173.61	1	0	181.97		
	4	229.60			175.61			183.97		
	6	231.60			177.61			185.97		
	8	233.60			179.61			187.97		
ATO reaction time [s]	**0.5**	227.60	1	0	173.61	1	0	179.99	1	0
	1	228.10			174.11			180.49		
	2	229.10			175.11			181.49		
	4	231.10			177.11			183.49		
	6	233.10			179.11			185.49		
	8	235.10			181.11			187.49		
Average braking rate of follower pod [m/s²]	**1.82**	227.60	75.85	186.55	173.61	76.74	188.72	179.99	16.01	39.37
	1.47	248.24			194.52			184.39		
	1.12	281.60			228.23			191.39		
	0.95	307.59			254.45			196.77		

In particular, we study three input parameters: communication delay, ATO reaction time and the braking rate of the follower pod. We do so for MB, $VC_{C/D}$ and VC_P. And this analysis is made for two types of braking: using reverse thrust and a constant braking rate. Our output parameter is the average minimum headway for all operational scenarios, switching technology and station layout.

III. CASE STUDY

We studied the capacity that the Hyperloop can safely provide for the different combinations of operational scenarios (Fig. 4) and technological configurations. The average time headways over all operational scenarios were considered for the signalling systems/modes and technological configurations (switching type with corresponding speed restriction, the number of chambers at stations and braking type/capability).

A. Sensitivity Analysis Results

The sensitivity analysis was performed for all the relevant combinations of operational scenarios and technological configurations reported previously in the Methodology. The capacity was assessed in terms of the time headway between consecutive capsules, where the highest capacity values correspond to the lowest time headways. The calculations considered the braking curves obtained from the simulation for the case of a flat track, for both types of braking. Fig. 2 exemplifies the braking curves obtained by reversing the motor for braking and using it at full power.

As mentioned before, we considered a range of values for both ATO reaction time and communication delay. These intervals start from the reference values for each case and up to 8 s. The fixed safety margin SM_0 has been considered between pods is 200 m if pods are moving and 50 m if pods are queueing behind each other when stopping at the same station platform. The braking rate of the leading pod is kept at the reference value, since our objective is to study how different braking abilities between vehicles affect capacity. A capsule length of 35 m is considered. The dwell time considered to embark/disembark passengers at stations is 120 s.

Tables I and II show the results of our sensitivity analysis, for the braking with a reverse thrust and using a constant braking rate, respectively. The results show how the minimum headways depend on the input parameters studied. The variation with communication headway and ATO reaction time is purely additive, of course. Still, we can see how large values for these parameters could considerably affect the minimum headways. For example, the minimum headways due to higher communication delays grow up to 4.4% when compared to the reference delay.

The braking rate capability of the follower pod has a higher influence on the headways. The difference of the braking rates does not impact all signalling systems/modes the same way. VCP is much less sensitive. MB and $VC_{C/D}$ are

TABLE II

MINIMUM TIME HEADWAYS [S] FOR ALL THE COMBINATIONS STUDIED WHEN USING A CONSTANT BRAKING RATE

		MB			$VC_{C/D}$			VC_P		
Input Parameter	X_i	Y_i	μ_i	σ_i	Y_i	μ_i	σ_i	Y_i	μ_i	σ_i
Average braking rate of follower pod [m/s²]	**2.45**	170.57	37.76	93.37	122.95	38.67	95.64	161.38	9.82	24.31
	2	182.52			135.15			164.46		
	1.5	204.04			157.18			170.01		
	1	245.54			199.94			181.12		

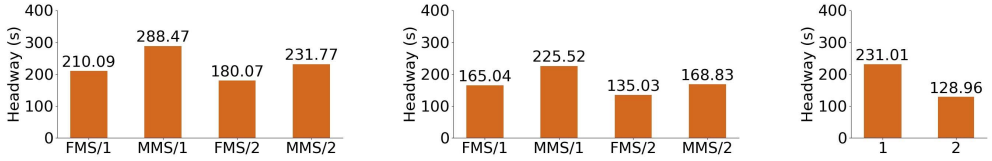

(a) (b) (c)

Fig. 7. Average time headways for different combinations of signalling system/mode, switch technology and number of airlocks/chambers at stations. Reverse thrust at full power used for braking. (a) MB. (b) $VC_{C/D}$. (c) VC_P.

similarly affected, as shown by the higher values of μ_i and σ_i. Therefore, capacity can be severely affected if pods with low braking rates coexist with more capable capsules. The results show clearly the added value of VC in comparison to MB. The minimum headways are always shorter when using this signalling system, hence VC outperforms MB by providing a higher transport capacity to the Hyperloop system.

B. Analysis of Reference Case

In addition to study the response of the outputs to variations of input parameters, it is important to analyze a specific configuration in detail. For that, we analyze one instance in which we assume all reference values for the input parameters. And we consider the case with reverse thrust for braking, with the follower pod using full power for reverse thrust. The results of such configuration are shown in Fig. 7. Again, we conclude that VC can clearly improve capacity over MB. There is no situation where MB can outperform VC.

Regarding the switching technology, we conclude that the MMS technology can bring relevant benefits if it becomes available. The fact pods do not need to reduce their speed when merging/diverging influences significantly the minimum headways at junctions.

The layout of stations plays also an important role on the overall capacity of the system. If pods are not able to perform passenger alighting/boarding operations simultaneously, this will represent a major capacity bottleneck, as this problem rapidly escalates with the number of pods, leading to very long headways and therefore a limited transport capacity.

We conclude that the highest capacity values are achieved by combining VC with the FMS technology and two chambers. This study shows that VC could provide substantial capacity improvements with respect to MB. The greatest improvements are obtained if VC could always be operated in the platooning mode, where an average time headway between pods of only 128.96 s could be achieved if an FMS is installed and considering two chambers. Such a setup would provide 27 pods/h meaning 810 pax/h/direction per tube. For the same switch technology and number of chambers, MB could only reach an average headway of 180.07 s meaning 19 pods/h and 570 pax/h/direction per tube. This represents a considerable increase of 42% in the number of pods/h.

TABLE III

COMPARISON OF TRANSPORT CAPACITY FOR DIFFERENT TRANSPORT MODES AND SYSTEM CONFIGURATIONS USING THE REFERENCE INPUT PARAMETERS

Transport mode and system configuration	Hourly transport capacity [veh/h]	Hourly transport capacity [pax/h]
Hyperloop with platooning, FMS and multiple station airlocks	27	810
Hyperloop with MB, MMS and single station airlock	19	570
Airplane [4]	-	312
High-speed railway [4]	12	9600

Van Goeverden *et al.* [5] estimated the transport capacity provided by the main alternatives to the Hyperloop, which corresponds to 9600 pax/h for the high-speed rail and 312 pax/h for the air passenger transport. This study shows that the Hyperloop could more than double the values of air transport but is far below the transport capacity of high-speed railways, even for the best technological configuration of virtually coupled platoons of pods, stations having multiple airlock/chambers to embark/disembark passengers simultaneously on/from different pods and junctions equipped with fixed magnetic switches requiring no speed reductions at the approach. This comparison of transport capacity for different transport modes and system configurations is summarized in Table III.

IV. Conclusion

This work provides a wide capacity analysis of the Hyperloop system for different signalling systems and considering several operational scenarios. Since the Hyperloop is still a concept for a new mode of transport, many different technologies have been proposed and it is not clear which might be available. For that reason, we performed a sensitivity analysis that allowed to study various possibilities.

The analysis has shown the concept of VC as the most suitable signalling system as it reduces the time headways between capsules, therefore increasing capacity. The fact capsules are separated by a relative instead of an absolute braking distance means shorter time headways can be achieved while using this technology.

This study shows that the reference headway values of 30 s claimed in the Hyperloop Alpha paper of Elon Musk [1] are not safely achievable even using advanced signalling systems. The only way to achieve those headways during peak hours would be by using braking rates of the pods that exceed 1g, which are unsafe and uncomfortable to passengers.

Furthermore, stations can severely reduce the capacity of the system in case pods are not allowed to stop at the same platform and embark/disembark passengers and cargo simultaneously. Unless more platforms can be used, each capsule would have to wait for the pod ahead to complete dwelling operations.

Further steps of this work should consider a wider range of possibilities for the Hyperloop system, e.g. in terms of the propulsion system. Also, studying capacity using simulation would allow a better comprehension of the dynamic interaction between vehicles, especially if more capsules and on-the-run platoon composition/decomposition under VC.

References

[1] *Hyperloop Alpha Document*, SpaceX, Hawthorne, CA, USA, 2013, p. 58.

[2] *Virgin Hyperloop–Passenger Test*. Accessed: Jul. 4, 2021. [Online]. Available: https://virginhyperloop.com/pegasus

[3] I. A. Hansen, "Hyperloop transport technology assessment and system analysis," *Transp. Planning Technol.*, vol. 43, no. 8, pp. 803–820, Nov. 2020, doi: 10.1080/03081060.2020.1828935.

[4] K. Decker *et al.*, "Conceptual feasibility study of the hyperloop vehicle for next-generation transport," in *Proc. AIAA 55th AIAA Aerosp. Sci. Meeting (SciTech Forum)*, 2017, pp. 1–22, doi: 10.2514/6.2017-0221.

[5] K. van Goeverden, D. Milakis, M. Janic, and R. Konings, "Analysis and modelling of performances of the HL (Hyperloop) transport system," *Eur. Transp. Res. Rev.*, vol. 10, no. 2, Jun. 2018, doi: 10.1186/s12544-018-0312-x.

[6] J. P. Powell and R. Palacín, "Passenger stability within moving railway vehicles: Limits on maximum longitudinal acceleration," *Urban Rail Transit*, vol. 1, no. 2, pp. 95–103, 2015, doi: 10.1007/s40864-015-0012-y.

[7] R. Pascoe and T. Eichorn, "What is communication-based train control?" *IEEE Veh. Technol. Mag.*, vol. 4, no. 4, pp. 16–21, Dec. 2009.

[8] G. Theeg and S. Vlasenko, *Railway Signalling and Interlocking*. Hamburg, Germany: Eurailpress, 2009.

[9] E. Quaglietta, "Analysis of platooning train operations under V2V communication-based signaling: Fundamental modelling and capacity impacts of virtual coupling," in *Proc. 98th Transp. Res. Board Annu. Meeting*, 2019, pp. 1–18.

[10] S. Gao, Y. Hou, H. Dong, S. Stichel, and B. Ning, "High-speed trains automatic operation with protection constraints: A resilient nonlinear gain-based feedback control approach," *IEEE/CAA J. Automatica Sinica*, vol. 6, no. 4, pp. 992–999, Jul. 2019, doi: 10.1109/JAS.2019.1911582.

[11] W. Chen, Q. Luo, W. Li, and L. Gong, "Optimization of capacity utilization of high-speed railway network," in *Proc. IEEE 5th Int. Conf. Intell. Transp. Eng. (ICITE)*, Sep. 2020, pp. 224–228, doi: 10.1109/ICITE50838.2020.9231332.

[12] E. Quaglietta, "A simulation-based approach for the optimal design of signalling block layout in railway networks," *Simul. Model. Pract. Theory*, vol. 46, pp. 4–24, Aug. 2014, doi: 10.1016/j.simpat.2013.11.006.

[13] S. Y. Choi *et al.*, "Sub-sonic linear synchronous motors using superconducting magnets for the hyperloop," *Energies*, vol. 12, no. 24, p. 4611, Dec. 2019, doi: 10.3390/en12244611.

[14] *406. Capacity*, UIC Leaflet, International Union of Railways, Paris, France, 2004.

[15] *Hyperloop Switch*. Accessed: Jul. 3, 2021. [Online]. Available: https://hardt.global/technology-development/

[16] W. Y. Ji, G. Jeong, C. B. Park, I. H. Jo, and H. W. Lee, "A study of non-symmetric double-sided linear induction motor for hyperloop all-in-one system (propulsion, levitation, and guidance)," *IEEE Trans. Magn.*, vol. 54, no. 11, Nov. 2018, Art. no. 8207304, doi: 10.1109/TMAG.2018.2848292.

[17] E. Quaglietta, M. Wang, and R. M. P. Goverde, "A multi-state train-following model for the analysis of virtual coupling railway operations," *J. Rail Transp. Planning Manage.*, vol. 15, Sep. 2020, Art. no. 100195, doi: 10.1016/j.jrtpm.2020.100195.

[18] J. Aoun *et al.*, "A hybrid delphi-AHP multi-criteria analysis of moving block and virtual coupling railway signalling," *Transp. Res. C, Emerg. Technol.*, vol. 129, Aug. 2021, Art. no. 103250, doi: 10.1016/j.trc.2021.103250.

[19] M. Wang, W. Daamen, S. P. Hoogendoorn, and B. van Arem, "Cooperative car-following control: Distributed algorithm and impact on moving jam features," *IEEE Trans. Intell. Transp. Syst.*, vol. 17, no. 5, pp. 1459–1471, May 2016, doi: 10.1109/TITS.2015.2505674.

[20] A. Ghasemi, R. Kazemi, and S. Azadi, "Stable decentralized control of a platoon of vehicles with heterogeneous information feedback," *IEEE Trans. Veh. Technol.*, vol. 62, no. 9, pp. 4299–4308, Nov. 2013, doi: 10.1109/TVT.2013.2253500.

[21] V. Milanés and S. E. Shladover, "Modeling cooperative and autonomous adaptive cruise control dynamic responses using experimental data," *Transp. Res. C, Emerg. Technol.*, vol. 48, pp. 285–300, Nov. 2014, doi: 10.1016/j.trc.2014.09.001.

[22] *HYPERNEX Deliverable D 2.1*, 2021.

[23] N. E. Lownes and R. B. Machemehl, "Sensitivity of simulated capacity to modification of VISSIM driver behavior parameters," *Transp. Res. Rec.*, vol. 1988, no. 1, pp. 102–110, vol. 2006, doi: 10.3141/1988-15.

[24] L. Leclercq, J. A. Laval, and N. Chiabaut, "Capacity drops at merges: An endogenous model," *Proc.-Social Behav. Sci.*, vol. 17, pp. 12–26, Jan. 2011, doi: 10.1016/j.sbspro.2011.04.505.

Rafael Mendes Borges received the M.Sc. degree in aerospace engineering from Instituto Superior Técnico, Lisbon, Portugal, in 2018. He was a Researcher at the Department of Transport and Planning, Delft University of Technology. His research interests include railway traffic optimization, predictive maintenance, and automatic railway operations.

Egidio Quaglietta received the Ph.D. degree in simulation-based signaling optimization. He is currently an Assistant Professor of railway traffic management at TU Delft. He is leading a research on virtual coupling for the Shift2Rail Project MOVINGRAIL. He has been intensively working in the field of railway signaling since 2008. He has worked as a Research and Development Engineer of several prominent railway companies, such as the Italian railway system supplier Ansaldo STS and the British railway infrastructure manager at Network Rail, where he led a workstream of the R&I Program "Digital Railway" as well as the sub-project on "Operations for Enhanced Capacity" for the EC FP7 Project Capacity for Rail (C4R). He has developed the simulation tool EGTRAIN. His main interests are in the areas of railway traffic and infrastructure optimization, innovative signaling technology, and automated railway operations. He is a member of the Institution of Railway Signal Engineers (IRSE).